Bulletin of JSME, Vol. 29, No. 254 August 1986

Paper No. 254—29

Temperature Distribution in the Vortex Flow Target System for Accelerator Breeder*

(Report 1. An analysis for the temperature distribution in the target and blanket irradiated with a proton beam)

By Kohshi MITACHI,** Hisanori TACHIBANA,*** and Kazuo FURUKAWA****

In the design of an accelerator breeder reactor, the most important problems are the radiation damage and the heat deposition in the target materials, which are irradiated with a high energy proton beam. To solve these problems, the vortex flow of molten salt was proposed as the target (and blanket) of the reactor.

An analytical study was conducted in this paper and the main concern was about the temperature fields within the target region of vortex flow. Rankin's vortex motion was assumed to calculate the velocity distribution in the target region. The temperature distributions and the maximum temperature of the target were obtained by a finite difference method. It was revealed that the present analysis was sufficient for the estimation of the maximum temperature. The radial distances between the beam and the vortex were varied and tested in order to lower the maximum temperature of the target, and the eccentric beam injection was found to be most effective.

Key Words : Thermal Engineering, Forced Convection Heat Transfer, Vortex Flow, Accelerator Breeder, Target System, Analysis

1. Introduction

The bombardment of high energy protons on the atomic nuclei induces the spallation reaction which generates many neutrons mainly by the evaporation process. An accelerator breeder concept utilizes this phenomenon in order to convert the fertile materials (^{232}Th or ^{238}U) into the fissile materials (^{233}U or ^{239}Pu). This breeder system has the following characteristics:

(i) One accelerator breeder using 300 mA beam of 1 GeV protons can efficiently produce a nuclear fuel sufficient to operate 5-15 fission power reactors of 1000 MWe size.

(ii) It is possible to utilize ^{232}Th and ^{238}U as new abundant nuclear energy resources.

(iii) The inventory of fissile material can be made small in contrast to the other breeder reactors such as liquid metal cooled fast breeder reactors.

(iv) Since it is operated in the subcritical conditions, the nuclear excursion never occurs.

In order to construct the accelerator breeder, research and development should be carried out in relation to (1) a high energy and high current accelerator and (2) a target (and blanket) system for the spallation reaction. Particularly in the target system, injection of the concentrated beam causes an extremely high temperature spot and the intensive proton and neutron fluxes inflict severe radiation damage to the target (and blanket) materials. In order to avoid these serious problems, adoption of a liquid target system seems to be indispensable [1-5].

The purpose of this study is to analyze the potential performance concerning the heat removal in the target system constructed of a molten salt, which is proposed by one of the authors [1-3,10-12]. A numerical simulation is performed to elucidate the temperature distribution and to estimate the maximum temperature in the target system.

2. Nomenclature

c_p : specific heat
d_b : diameter of proton beam
g : gravitational acceleration
q : flow rate per unit depth of target
r : radial coordinate (see Fig.2)
r_1 : radius corresponding to half width of vortex ($r \to r_1$, $V_\phi \to V_{\phi m}$)
r_2, r_c : core radius of swirling flow
r_b : injection position of proton beam
r_v : radius of free surface of vortex

* Received 21st November 1984
** Associate Professor, *** Graduate Student, Toyohashi University of Technology, Toyohashi, 440 Japan.
**** Professor, Tokai University, Hiratsuka, 259-12 Japan.

T : temperature
ΔT_b : maximum temperature rise
V_r, V_ϕ, V_z : velocities in r, ϕ and z directions
$V_{\phi m}$, V_{rm} : maximum values of V_ϕ and V_r
W_b : heat generated by proton beam
Z : axial coordinate (see Fig.2)
Z_0 : depth of vortex
Z_b : depth of heating zone
ρ : density
ϕ : azimuth (see Fig.2)

3. Analysis

3.1 Target system

In order to elucidate the analytical model of the target system under consideration, a schematic diagram of the accelerator molten salt breeder is depicted in Fig.1. The size of target salt bath containing Th is about 5 m in diameter and 6 m in depth. Inside of the reactor vessel 4 made of Hastelloy N is covered with thick graphite blocks 5&6 for the neutron shielding. The target salt is introduced from the upper part 2 of the vessel and it forms a narrow vortex of about 1 m depth on the salt surface. The proton beam of about 1 GeV is directly radiated through this vortex and the spallation reaction takes place in the central part of the salt bath.

There have been several proposals for the target system of solid materials [4,5,8,9]. Comparing those proposals, the liquid target system which utilizes a swirling flow of molten salt shown in Fig.1 seems to solve many technical troubles such as the concentration of heat generation, the radiation damage and the necessity of shuffling of the blanket materials.

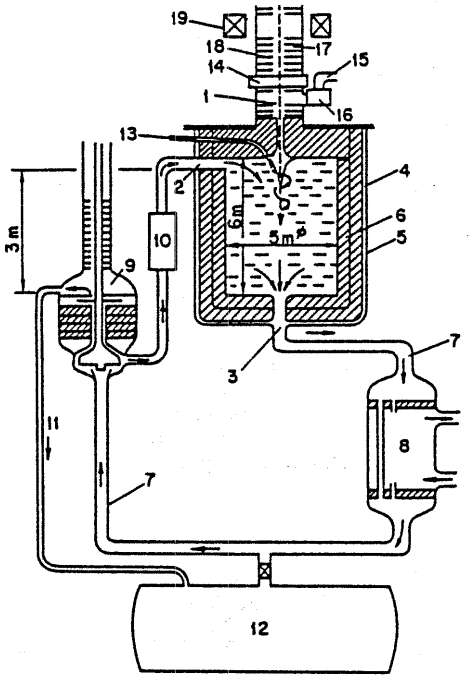

Fig.1 Schematic diagram of accelerator molten salt breeder

1 proton beam, 2 salt inlet, 3 salt outlet, 4 reactor vessel, 5&6 graphite, 7 primary loop, 8 heat exchanger, 9 main pump, 10 throttle valve, 11 over flow line, 12 storage tank, 13 high pressure salt outlet, 14 gate valve, 15 vacuum line, 16 vapor trap, 17 duct, 18 orifice, 19 focussing magnet.

3.2 Numerical analysis of temperature profile

3.2.1 Governing equations

A schematic diagram of the target and that of its coordinate system are depicted in Fig.2. The conservation of energy dictates

$$\rho c_p \left(V_r \frac{\partial T}{\partial r} + \frac{V_\phi}{r}\frac{\partial T}{\partial \phi} + V_z \frac{\partial T}{\partial Z}\right) = \lambda\left(\frac{\partial^2 T}{\partial r^2} + \frac{1}{r}\frac{\partial T}{\partial r} + \frac{1}{r^2}\frac{\partial^2 T}{\partial \phi^2} + \frac{\partial^2 T}{\partial Z^2}\right) + W \quad ..(1)$$

where the flow and temperature profiles are supposed to be steady and the physical properties of the fluid to be constant. The rate of heat generation W caused by the proton irradiation is unknown at present, but it is considered to be independent of Z [7]. In the present study, therefore, the rate of heat generation W is assumed to be constant throughout the cylindrical region of diameter d_b and depth Z_b.

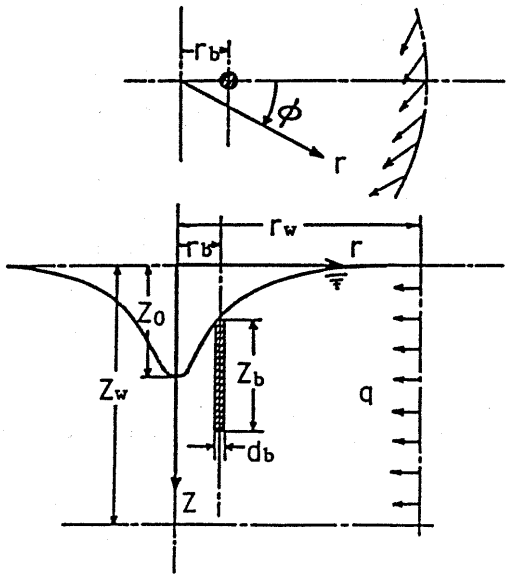

Fig.2 Coordinate system

$$W = \frac{W_b}{\frac{\pi}{4} d_b^2 Z_b} \quad \cdots\cdots\cdots\cdots\cdots\cdots\cdots\cdots (2)$$

The boundary conditions are as follows.

$$\left.\begin{aligned} T &= 0 \quad \text{at} \quad r = r_w \quad \text{and} \quad 0 \leqq Z \leqq Z_w \\ \frac{\partial T}{\partial Z} &= 0 \quad \text{at} \quad 0 \leqq r \leqq r_w \quad \text{and} \quad Z = Z_w \end{aligned}\right\} \cdots\cdots (3)$$

On the free surface, the heat flux is assumed to be zero in the normal direction.

The numerical analysis is performed in the region of $0 \leqq r \leqq r_w$ and $0 \leqq Z \leqq Z_w$, where r_w and Z_w are taken large enough compared with r_b so that the effect of the flow boundaries is negligible in the calculated results.

3.2.2 Velocity distribution

From the previous experiments [10-12] for swirling flow and Ogawa's experiments [13] for cyclone separator, the velocity distribution in the target system becomes as follows:

(i) at $r_v \leqq r \leqq r_1$

$$\left.\begin{aligned} \frac{V_\phi}{V_{\phi m}} &= \frac{r}{r_1}, \quad V_z = \frac{qZ}{\pi r_2^2}, \\ V_r &= -\frac{q(r^2 - r_v^2)}{2\pi r_2^2 r}, \quad V_{\phi m} = \sqrt{gZ_0} \end{aligned}\right\} \cdots (4)$$

$$\text{if} \quad Z \geqq Z_0, \quad r_v = 0$$

Table 1. Dimensions of target system

Heating zone by proton beam	
heat deposition	W_b=300 MW
diameter	d_b= 10 cm
length	Z_b= 1.2 m
injection position	r_b= 0.3 m
Flow field	
vortex depth	Z_0= 1.5 m
vortex width	r_1= 0.3 m
core radius	r_c= 1.0 m
flow rate	q = 5.0 m^2/s

Table 2. Physical properties of $LiF-BeF_2-ThF_4-^{233}UF_4$ systems at 913K (64 - 18 - 17.5 - 0.5 mol%)

density	ρ = 2.70	t/m^3
specific heat	c_p= 1.36	MJ/(tK)
conductivity	λ = 1.2x10^{-6}	MJ/(mK)

(ii) at $r_1 < r \leqq r_c$

$$\left.\begin{aligned} \frac{V_\phi}{V_{\phi m}} &= \frac{r_1}{r}, \quad V_z = \frac{qZ}{\pi r_2^2} \\ V_r &= -\frac{q(r^2 - r_2^2)}{2\pi r_2^2 r} \end{aligned}\right\} \cdots\cdots (5)$$

where $r_c = \sqrt{r_2^2 + r_v^2}$

(iii) at $r > r_c$

$$\left.\begin{aligned} \frac{V_\phi}{V_{\phi m}} &= \frac{r_1}{r}, \quad V_z = 0, \\ V_r &= -\frac{q}{2\pi r} \end{aligned}\right\} \cdots\cdots (6)$$

At radius r_w, the target salt is supplied uniformly with the flow rate q m^3/s per every 1 m depth. The salt swirls horizontally in the peripheral region, and at the same time it flows in Z direction in the core region. The velocity component V_ϕ is assumed to obey Rankin's vortex rule, which is the maximum velocity $V_{\phi m}$ lying at the radius r_1.

The shape of the vortex, i.e., the coordinates of the free surface r_v and Z_v are determined considering V_ϕ only for the sake of simplicity as follows:

(i) at $r_v \leqq r_1$

$$Z_v = Z_0 \left[1 - \frac{1}{2} \left(\frac{r_v}{r_1}\right)^2 \right] \quad \cdots\cdots (7)$$

(ii) at $r_v > r_1$

$$Z_v = \frac{1}{2} Z_0 \left(\frac{r_1}{r_v}\right)^2 \quad \cdots\cdots\cdots\cdots (8)$$

3.2.3 Numerical procedure

The finite difference method is used to solve the governing equation, Eq.1, subject to the boundary conditions, Eq.3.

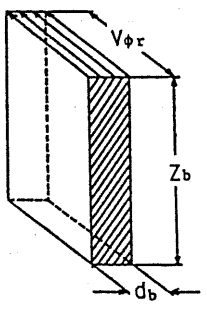

Fig.3 Calculation model for approximate theory

The diffusion terms and the convection terms in Eq.1 are calculated using the second order central and upstream differences, respectively. The latter differentiation method saves the computing time. The resultant equation is solved by SOR method.

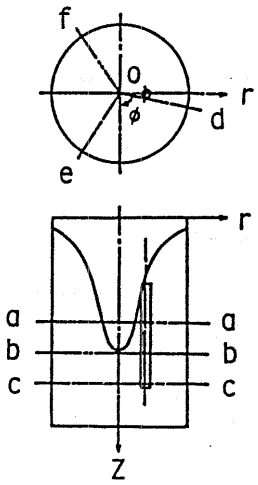

Fig.4 Region of numerical calculation

Table 1 lists the heat generation W_b, the beam diameter d_b and the vortex depth Z_0, which are given in the conceptual design [7,10,11,12]. Calculations make clear the effect of these design parameters on the temperature distribution. LiF- BeF_2- ThF_4- $^{233}UF_4$ systems is taken as the target salt and the composition and thermophysical properties are listed in Table 2 [3,7].

3.3 Approximate theory of maximum temperature rise

If the temperature of the target salt rises uniformly by ΔT_b when the salt flows through the heating zone with the velocity

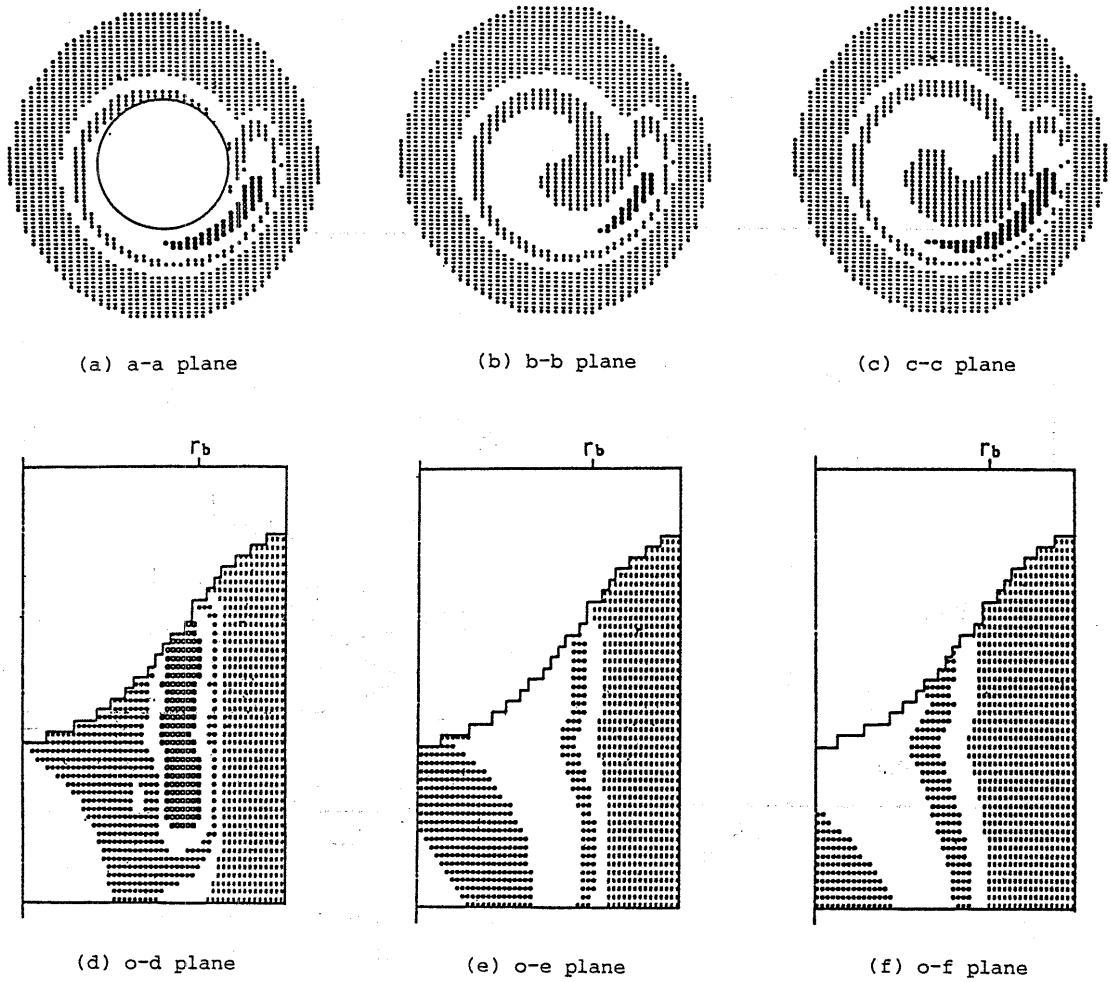

Fig.5 Temperature profiles in target system

$V_{\phi r}$ as shown in Fig.3, the following relationship between W_b and ΔT_b holds.

$$\left.\begin{aligned} &\rho c_p Z_b d_b V_{\phi r} \Delta T_b = W_b \\ &V_{\phi r} = \sqrt{V_\phi^2 + V_r^2} = V_\phi \sqrt{1+\zeta} \\ &\zeta = (V_r / V_\phi)^2 \end{aligned}\right\} \quad \cdots\cdots\cdots\cdots (9)$$

where the heating parameter ΔT_0 is defined as follow:

$$\Delta T_0 = \frac{W_b}{\rho c_p Z_b d_b \sqrt{g Z_0}} \quad \cdots\cdots\cdots\cdots (10)$$

By substituting Eq.4 - Eq.6 into Eq.9, the maximum temperature rise ΔT_b can be obtained from the beam radiation position r_b as follows:

(i) if $r_b \leq r_1$,

$$\left.\begin{aligned} &\Delta T_b = \frac{\Delta T_0}{\sqrt{1+\zeta}} \left(\frac{r_1}{r_b}\right) , \\ &\zeta = \frac{1}{4\pi^2} \left(\frac{r_1}{r_2}\right)^4 \left(\frac{q}{r_1 \sqrt{g Z_0}}\right)^2 \end{aligned}\right\} \quad \cdots\cdots\cdots (11)$$

(ii) if $r_1 < r_b \leq r_2$,

$$\left.\begin{aligned} &\Delta T_b = \frac{\Delta T_0}{\sqrt{1+\zeta}} \left(\frac{r_b}{r_1}\right) , \\ &\zeta = \frac{1}{4\pi^2} \left(\frac{r_1}{r_2}\right)^4 \left(\frac{r_b}{r_1}\right)^4 \left(\frac{q}{r_1 \sqrt{g Z_0}}\right)^2 \end{aligned}\right\} \quad \cdots (12)$$

(iii) if $r_b > r_2$,

$$\left.\begin{aligned} &T_b = \frac{\Delta T_0}{\sqrt{1+\zeta}} \left(\frac{r_b}{r_1}\right) \\ &\zeta = \frac{1}{4\pi^2} \left(\frac{q}{r_1 \sqrt{g Z_0}}\right)^2 \end{aligned}\right\} \quad \cdots\cdots\cdots (13)$$

One of the technical troubles supposed to occurs in the target system is the local and extreme temperature rise due to the concentrated heat generation by the proton radiation. The temperature rise may cause an explosive evaporation of the target salt. The effect of each design parameter on the maximum temperature rise can be estimated by Eq.11 - Eq.13. Hence, an approximate theory is useful and convenient in order to estimate the maximum temperature. However, the precise calculation should be performed when more detailed knowledge of the temperature profile is required.

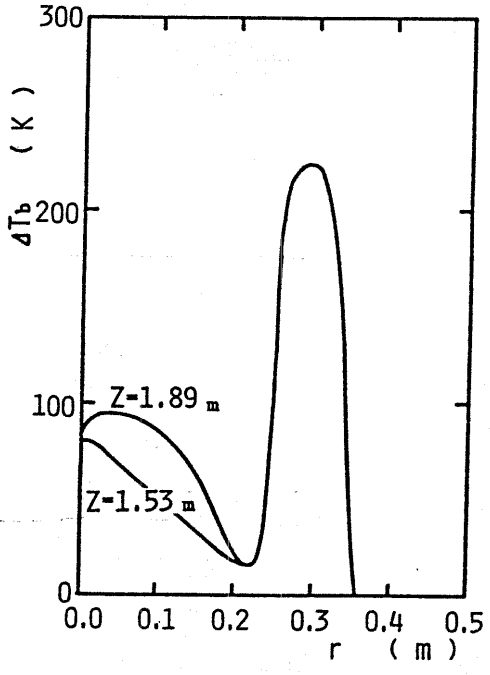

W_b=300MW, Z_0=1.5m, q=5.0m²/s
ϕ=10°, r_1=r_b=0.3m, r_2=1.0m

Fig.6 Temperature distribution in Z direction

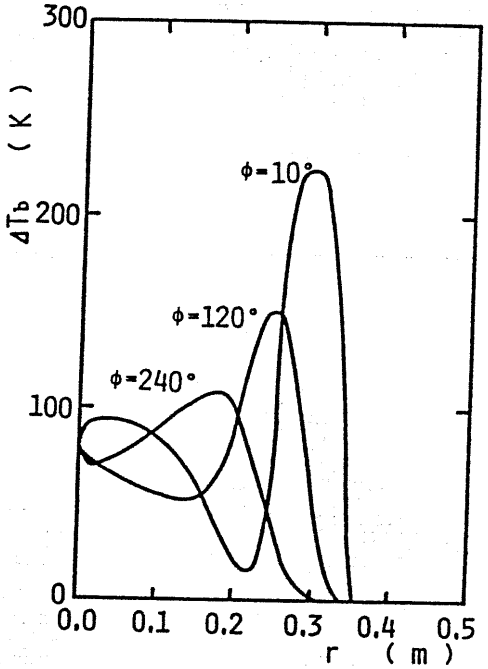

W_b=300MW, Z_0=1.5m. q=5.0m²/s
Z=1.89m, r_1=r_b=0.3m, r_2=1.0m

Fig.7 Temperature distribution in ϕ direction

4. Results and Discussion

4.1 Temperature distribution

Numerical calculations are performed on the case of 300 MW beam heating. Typical results of the temperature profile in the target system are shown in Fig.5;

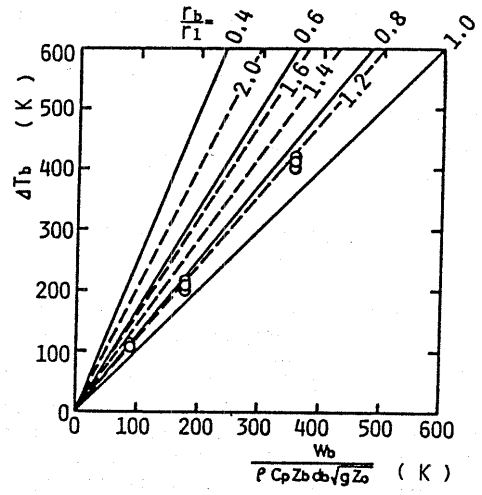

——— approximate theory ($r_b \leq r_1$)
----- approximate theory ($r_b \geq r_1$)
○ numerical result

Fig.8 Maximum temperature rise (ζ=0)

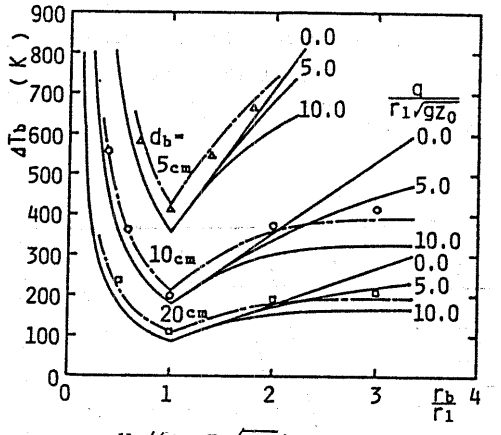

$W_b/(\rho c_p Z_b \sqrt{gZ_0})$=17.8mK,
Z_0/r_1=5.0, r_2/r_1=3.3

——— approximate theory
——— (approximate theory $q/r_1\sqrt{gZ_0}$=10) x 1.2

△ d_b= 5cm
○ d_b=10cm
□ d_b=20cm
} numerical result

Fig.9 Maximum temperature rise in relation to beam radiation position

The design conditions are listed in Table 1 [7,11,12].

Fig.5.a, 5.b and 5.c are the temperature profiles on the horizontal cross sections, and Fig.5.d, 5.e and 5.f are the temperature profiles on the vertical cross sections through Z axis as depicted in Fig.4. In this way, the temperature profile exhibits a swirling motion of the target salt. The hottest spot arises just behind the cylindrical heating zone.

Fig.6 shows the radial temperature distributions at the depth z (1.17, 1.53 and 1.89m) and at ϕ = 10° (o-d plane in Fig.4). The temperature distribution for Z = 1.17m is omitted in the figure, because it coincides with those for Z = 1.53m or 1.89m in the region of r ≥ 0.2m. Moreover, the target salt does not exist at that depth in the region of r < 0.2m. The temperature profiles have a sharp peak and their shapes are similar to each other in the vicinity of the heating zone, irrespective of the difference in the depth.

The change of the temperature distribution with ϕ on c-c plane in Fig.4 is shown in Fig.7. A sharp peak for ϕ = 10 is attenuated by the swirling motion of the target salt.

4.2 Maximum temperature rise

4.2.1 Effect of beam diameter, depth of heating zone and depth of vortex

In an ordinary design condition in which the flow rate is not large, V_r is so

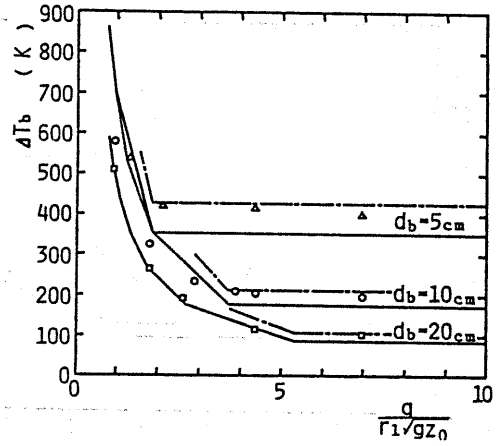

$W_b/(\rho c_p Z_b \sqrt{gZ_0})$=17.8mK,
Z_0/r_1=5.0, r_b/r_1=1.0, r_2/r_1=3.3

——— approximate theory
——— (approximate theory) x 1.2

△ d_b= 5cm
○ d_b=10cm
□ d_b=20cm
} numerical result

Fig.10 Maximum temperature rise in relation to flow rate

small in comparison with V_ϕ that ζ in Eq.11 - Eq.13 becomes very small. The relationship between the maximum temperature rise ΔT_b and the heating parameter $W_b/(\rho c_p Z_b d_b \sqrt{gZ_0})$ are shown in Fig.8, where the solid and broken lines are obtained from the approximate theory for the cases of $r_b \leq r_1$ and $r_b > r_1$, respectively. Even if the same amount of heat W_b is deposited in the target salt, the maximum temperature rise ΔT_b decreases with an increase of the beam diameter d_b, the depth of heating zone Z_b and the depth of vortex Z_0. The marks O in the figure designate numerical results for the cases of $r_b/r_1 = 1.0$ and $q/(r_1\sqrt{gZ_0}) = 2.0 - 7.0$. The maximum temperature rise ΔT_b obtained from the approximate theory is smaller, by about 20%, than the numerical results.

4.2.2 Effects of beam radiation position

The relation between the maximum temperature rise ΔT_b and the dimensionless position of beam radiation r_b/r_1 is shown in Fig.9, where △, O and □ indicate the numerical results obtained for the beam diameters 5, 10 and 20cm, respectively. The solid lines represent the correlations from the approximate theory, and for $q/(r_1\sqrt{gZ_0}) = 10$ the broken lines are located 1.2 times higher than the solid lines in order to adjust the difference between the exact and approximate calculations. As shown in the figure, the eccentric beam radiation is most effective in order to lower the maximum temperature rise ΔT_b. From a viewpoint of thermal engineering, the optimum position of beam radiation r_b should be set at r_1, which corresponds to half width of the vortex. When the beam is radiated at other positions, especially at a radius smaller than r_1, the target salt is overheated. For example, ΔT_b is estimated at 220K under the conditions of Table 1 and $r_b = r_1$; when the beam is radiated at the center of the swirling flow, ΔT_b increases to 3200K.

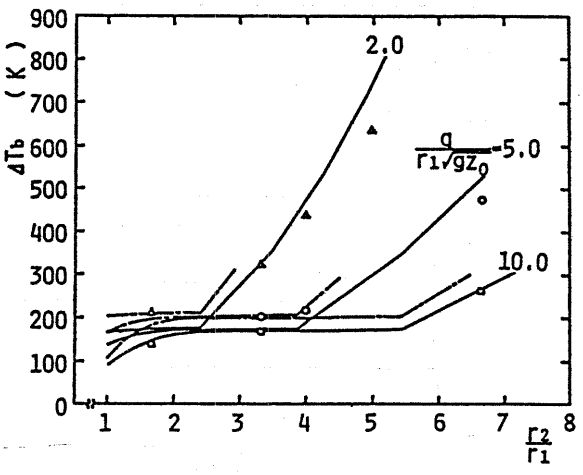

$W_b/(\rho c_p Z_b d_b \sqrt{gZ_0}) = 178K$,
$z_0/r_1 = 5.0$, $r_b/r_1 = 1.0$

——— approximate theory
—·— (approximate theory) x 1.2
△ $q/(r_1\sqrt{gZ_0}) = 2.0$
O $q/(r_1\sqrt{gZ_0}) = 5.0$
□ $q/(r_1\sqrt{gZ_0}) = 10.0$
} numerical result

Fig.11 Maximum temperature rise in relation to core radius

4.2.3 Effects of flow rate and core radius

The relation between the maximum temperature rise ΔT_b and the dimensionless flow rate $q/(r_1\sqrt{gZ_0})$ is shown in Fig.10, where △, O and □ indicate the numerical results for the beam diameters 5, 10 and 20cm, respectively. The solid lines are obtained from the approximate theory and the broken lines are drawn 1.2 times higher than the solid lines taking into account the difference between the exact and approximate calculations.

In the region of larger flow rates, the maximum temperature rise ΔT_b remains almost unchanged. But in the region where $q/(r_1\sqrt{gZ_0})$ is smaller than the critical amount, ΔT_b increases drastically with a decreasing flow rate. The increase of ΔT_b is caused by the fact that the heated salt circulates to the heating zone in the case of small flow rate or small V_r.

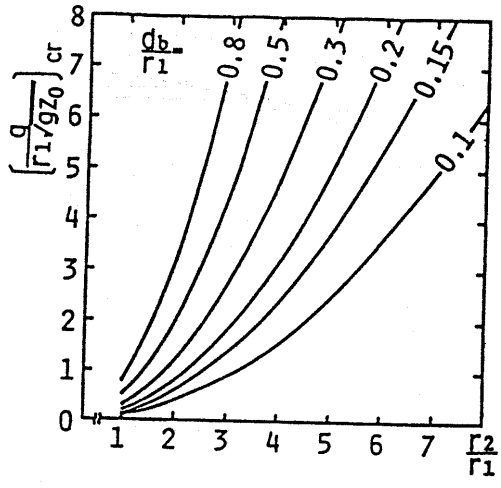

$r_b/r_1 = 1.0$

Fig.12 Critical flow rate

Fig.11 shows the effect of the dimensionless core radius r_2/r_1 on ΔT_b. The marks △, O and □ indicate the numerical results and the solid lines are obtained from the approximate theory. The broken lines are drawn 1.2 times higher than those of the approximate theory. As shown in the figure, ΔT_b changes only a little in the range of smaller r_2/r_1, but it increases rapidly with an increasing r_2/r_1 in the range of larger core radii. The reason is almost the same as in the case of Fig.10. Even if the flow rate is kept constant, V_r decreases with an increase of the core radius, so that the salt, once heated, returns to the same place after circulation.

The correlations between the core radius r_2/r_1 and the dimensionless critical flow rate $q/(r_1\sqrt{gz_0})_{cr}$ at which ΔT_b begins to increase rapidly are obtained from the equation of the velocity distribution as shown in Fig.12. In the design of target system of the accelerator breeder, $q/(r_1\sqrt{gz_0})$ must be kept large than the critical amount. In order to realize this condition, it would be necessary to make not only the flow rate in the core region large enough by setting the core radius small, but also recirculate the low temperature salt near the exit toward the upper region of the target system.

5. Conclusions

Numerical calculations are performed to obtain the temperature profile in the target (and blanket) system of the accelerator molten salt breeder. The following results are obtained:

(1) The eccentric beam radiation is most effective in order to lower the maximum temperature of the salt. The optimum radial distance between the beam and the vortex becomes equal to r_1, which corresponds to the half width of the vortex.

(2) The maximum temperature of the target remains constant when a larger than critical amount of the target salt is supplied. But it begins to rise rapidly if the flow rate is set smaller than the critical amount.

(3) The smaller core radius of the swirling flow is recommendable in order to keep the flow rate effectively larger than the critical amount.

(4) The approximate theory derived in the present study is useful to estimate the maximum temperature of the target system.

The authors wish to express their thanks to Mr. N. Nakamura, Ishikawajima Harima Heavy Industry Co., for his valuable suggestions and discussions.

References

1. K. Furukawa, et al., J. Nucl. Technol., 18(1981),p.79.
2. K. Furukawa, et al., Proc. 4th Int. Coll. Adv. Neutron Source (1981) p.349.
3. k. Furukawa, et al., Proc. Japan - U.S. Seminar on Thorium Fuel Reactor, (1982).
4. The Research Committee of Thorium Cycle, Thorium Cycle (in Japanese), (1980), p.183.
5. The Research Committee of Neutron Target System, J. Atomic Energy Soci. Japan (in Japanese), Vol.25, No.5 (1983), p.344.
6. M. Odera, J. Atomic Energy Soci. Japan (in Japanese), Vol.26, No.6 (1984), p.474.
7. Preprint of the Committee of Molten Salt Reactor (in Japanese), (1984).
8. H. Takahashi, J. Atomic Energy Soci. Japan (in Japanese), Vol.21, No.5 (1979), p.397.
9. F. R. Mynatt, et al., ORNL/TM-5750 (1979).
10. K. Mitachi, et al., Proc. 19th National Heat Transfer Symposium of Japan (in Japanese), (1982), p.115.
11. K. Mitachi, et al., Proc. the annual meeting of the Atomic Energy Society of Japan (in Japanese), (1983), p.214.
12. K. Mitachi, et al., ibid, (1984), p.212.
13. H. Ogawa, Uzugaku (in Japanese) (1981), p.110, Sankaido.